

## Secure Integrated Sensing and Communication Systems Assisted by Active RIS

Zheng Yang <sup>ID</sup>, Member, IEEE, Siyu Zhang <sup>ID</sup>,  
 Gaojie Chen <sup>ID</sup>, Senior Member, IEEE,  
 Zhicheng Dong <sup>ID</sup>, Member, IEEE, Yi Wu <sup>ID</sup>, Member, IEEE,  
 and Daniel Benevides da Costa <sup>ID</sup>, Senior Member, IEEE

**Abstract**—In this paper, we investigate secure transmission in active reconfigurable intelligent surface (RIS)-assisted integrated sensing and communication (ISAC) systems. The dual-function base station communicates with the legitimate user and detects the sensing target simultaneously via active RIS, while the communication signal is intercepted by a potential eavesdropper (Eve). To achieve secure transmission, a novel successive interference cancellation scheme is proposed, where the sensing signal can disrupt the potential eavesdropping while keeping the legitimate user link intact. Then, the secure rate maximization problem is proposed, where the active beamforming of the RIS, the legitimate user's transmit beamforming, the Eve's transmit beamforming, and the radar receive beamforming are jointly optimized. However, the secure rate expression is non-convex, an iteration optimization algorithm based on majorization-minimization method and semi-definite programming are proposed to decompose the original problem into three sub-problems. Simulation results illustrate that the secrecy performance of the proposed scheme outperforms the passive RIS-assisted ISAC systems and the traditional cellular networks aided by active RIS.

**Index Terms**—Active reconfigurable intelligent surface (RIS), integrated sensing and communication (ISAC), secure transmission, semi-definite programming.

### I. INTRODUCTION

Secure transmission will continue to be a challenging problem in next generation mobile communication networks, since wireless channels provide an open or unsecured medium where transmitted signals are easy to be intercepted by the potential eavesdroppers (Eves) [1]. The

Received 9 April 2024; revised 10 July 2024; accepted 24 August 2024. Date of publication 27 August 2024; date of current version 19 December 2024. The work of Zheng Yang, Siyu Zhang, and Yi Wu was supported in part by the Natural Science Foundation of Fujian Province under Grant 2022J01169, in part by the Fujian Province Special Fund Project for Promoting High-Quality Development of Marine and Fisheries Industries, under Grant FJHYF-ZH-2023-03, and in part by the Fujian Provincial Direct Unit Special Project for Education and Research, Fujian Financial Referral [2023] No. 834. The work of Zhicheng Dong was supported by the Science and Technology Major Project of Tibetan Autonomous Region of China under Grant XZ202201ZD0006G04 and in part by the Lhasa Science and Technology Plan Project under Grant LSKJ202405. The work of Gaojie Chen was supported by the Fundamental Research Funds for the Central Universities, Sun Yat-sen University, under Grant 24hytd010. The review of this article was coordinated by Dr. Trung Q. Duong. (*Corresponding authors: Zhicheng Dong; Yi Wu.*)

Zheng Yang, Siyu Zhang, and Yi Wu are with the College of Photonic and Electronic Engineering, Fujian Normal University, Fuzhou 350117, China (e-mail: zhengyang@fjnu.edu.cn; zsyfjnu@163.com; wuyi@fjnu.edu.cn).

Gaojie Chen is with the School of Flexible Electronics (SoFE), Sun Yat-sen University, Shenzhen 518107, China (e-mail: gaojie.chen@ieee.org).

Zhicheng Dong is with the School of Information Science and Technology, Tibet University, Lhasa 850011, China (e-mail: dongzc666@163.com).

Daniel Benevides da Costa is with the Interdisciplinary Research Center for Communication Systems and Sensing (IRC-CSS), Department of Electrical Engineering, King Fahd University of Petroleum & Minerals (KFUPM), Dhahran 31261, Saudi Arabia (e-mail: danielbcosta@ieee.org).

Digital Object Identifier 10.1109/TVT.2024.3450792

key idea of integrated sensing and communication (ISAC) is that both communication and sensing functions are integrated within the same hardware system, which can enable secure transmission by utilizing sensing targets to disrupt the Eves [2]. Furthermore, the active reconfigurable intelligent surface (RIS) is designed with numerous low-power consumption units, each equipped with a dedicated amplifier not only enables versatile signal manipulation but also plays a significant role in improving the reliability and security of communication systems [3]. Therefore, applying active RIS within ISAC systems holds promise for enhancing security operations, which can further improve the secrecy performance.

In [4], the authors focused on maximizing the signal-to-interference-plus-noise ratio (SINR) in passive RIS-assisted multiple-input multiple-output ISAC systems with an eavesdropping sensing target, where the transmit beamforming vectors and the phase shifts of the passive RIS were jointly designed. In [5], the primary objective was to minimize the maximum eavesdropper's SINR in passive RIS-aided secure ISAC systems, where the active beamforming at the BS and the passive beamforming at the RIS were jointly designed. In [6], the achievable sum secrecy rate maximization problem was proposed to joint optimize the active and passive beamforming vectors in passive RIS-assisted ISAC systems with the additional aid of artificial noise. The works in [4], [5], [6] primarily focused on the passive RIS-assisted ISAC systems, without fully exploring the potential of active RIS and sensing target to further enhance secure performance. In [7], the authors aimed to maximize the radar signal-to-noise ratio (SNR) in active RIS-assisted ISAC systems, emphasizing the joint optimization of the transmit beamforming vectors of the communication and sensing, and the active beamforming of the RIS. In [8], the authors proposed the active RIS to maximize the secure rate in multiple-input single-output ISAC systems with an eavesdropping sensing target, by jointly optimizing the radar receive filter, the active RIS reflection coefficients matrix, and the transmitter's beamformers. The active RIS was applied into ISAC systems in [7] and [8], but both sensing and communication signals were transmitted using different beamforming vectors, the mixing of these signals can indeed impact the overall system performance, particularly the sensing signal will affect the communication quality and reliability. The key idea of this paper is to exploit the active RIS to design a novel SIC scheme that the sensing signal can be successfully removed before evaluating the communication performance, while the sensing target is regarded as a cooperative jamming that can remarkably deteriorate the performance of Eves.

Motivated by the above discussion, we propose to design a novel successive interference cancellation (SIC) decoding order scheme to enhance the secure transmission in ISAC systems assisted by active RIS. Specifically, the SIC decoding order is designed based on communication beamforming and sensing beamforming, which can achieve the results that the sensing signal can be successfully removed by legitimate user before decoding its own message while the sensing signal is regarded as interference when the Eve decodes legitimate user's signal. Then, we formulate the secure rate maximization problem, subject to the proposed SIC decoding order, the radar SNR constraint, and the maximum transmit and amplification power budget at the BS and the active RIS, respectively. Furthermore, we propose an alternating optimization algorithm to solve the non-convex secure rate problem, by using the methods of majorization-minimization (MM) and semi-definite programming (SDP). Simulation results demonstrate the proposed scheme with SIC decoding order can remarkably improve

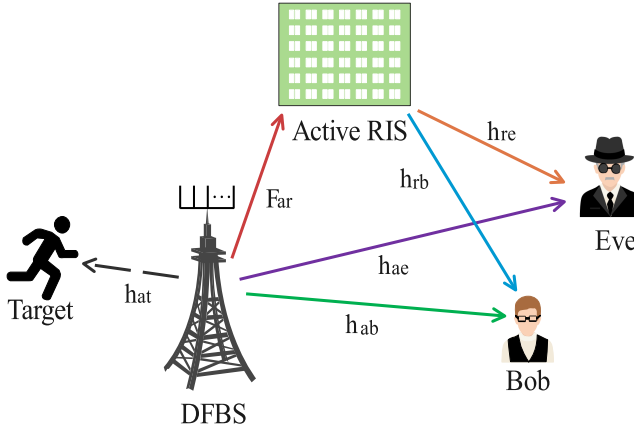


Fig. 1. Secure transmission of ISAC systems aided by active RIS.

the secure rate, compared to the active RIS-aided traditional cellular communication networks and the passive RIS-aided ISAC systems.

## II. SYSTEM MODEL

We consider an ISAC system aided by an active RIS consisting of  $N$  units as depicted in Fig. 1, which contains one dual-function base station (DFBS) with  $M$  transmit/receive antennas, one legitimate user (Bob) with single antenna, one potential Eve with single antenna,<sup>1</sup> and one sensing target. The DFBS communicates with the Bob and detects the sensing target simultaneously, while the Eve can eavesdrop Bob's message. Assumed that the sensing target is near to the DFBS, but is far away from the active RIS. In this scenario, the line-of-sight links between the DFBS and the sensing target are strong, while the links from the DFBS to the sensing target via the RIS are relatively poor and can be omitted [9]. The main reason is that the received echo signal at the DFBS via RIS is significantly affected by the distances from the DFBS to the RIS, from the RIS to the sensing target, and from the DFBS to the RIS, which leads to the results that the received echo signal is quite poor, compared to the received echo signal directly from the sensing target.

### A. Communication Signal Model

Let  $\mathbf{w}_b \in \mathbb{C}^{M \times 1}$  and  $\mathbf{w}_t \in \mathbb{C}^{M \times 1}$  denote the transmit beamforming vectors for the Bob and target, respectively. Furthermore, let  $x_b$  and  $x_t$  denote the communication and sensing signals for the Bob and target, respectively. According to downlink non-orthogonal multiple access (NOMA) scheme, the transmit signals  $x_b$  and  $x_t$  can be mixed together by the DFBS, which can be expressed as follows:

$$\mathbf{x} = \mathbf{w}_b x_b + \mathbf{w}_t x_t. \quad (1)$$

Note that the active RIS is used to help the DFBS reflect the mixed signal  $\mathbf{x}$  in (1) to the Bob, the received signal at the Bob and the Eve can be expressed as follows:

$$\begin{aligned} y_i &= \mathbf{h}_{ai}^H \mathbf{x} + \mathbf{h}_{ri}^H \Theta (\mathbf{F}_{ar} \mathbf{x} + \boldsymbol{\omega}_r) + \boldsymbol{\omega}_i \\ &= (\mathbf{h}_{ai}^H + \mathbf{h}_{ri}^H \Theta \mathbf{F}_{ar}) \mathbf{x} + \mathbf{h}_{ri}^H \Theta \boldsymbol{\omega}_r + \boldsymbol{\omega}_i \\ &= \mathbf{g}_i (\mathbf{w}_b x_b + \mathbf{w}_t x_t) + \mathbf{h}_{ri}^H \Theta \boldsymbol{\omega}_r + \boldsymbol{\omega}_i, \quad i \in \{b, e\}, \end{aligned} \quad (2)$$

<sup>1</sup>For a potential Eve with multiple antennas, the eavesdropping rate can be higher. Note that the sensing target is regarded as a cooperative jamming, and the DFBS must allocate more transmit power to the sensing target to decrease the eavesdropping rate. We will consider this interesting direction in future work.

where  $\mathbf{g}_i = \mathbf{h}_{ai}^H + \mathbf{h}_{ri}^H \Theta \mathbf{F}_{ar} \in \mathbb{C}^{M \times 1}$ ,  $\mathbf{h}_{ai} \in \mathbb{C}^{M \times 1}$ ,  $\mathbf{h}_{ri} \in \mathbb{C}^{N \times 1}$ , and  $\mathbf{F}_{ar} \in \mathbb{C}^{N \times M}$  denote the channels from the DFBS to the Bob (Eve), from the active RIS to the Bob (Eve), and from the DFBS to the active RIS, respectively.  $\Theta = \text{diag}(\sqrt{\beta_1} e^{j\theta_1}, \dots, \sqrt{\beta_N} e^{j\theta_N})$  represents the reflection coefficient matrix of the active RIS, where  $\beta_n \in [0, \tau_n]$  and  $\theta_n \in [0, 2\pi]$  denote the amplitude and phase shift of the  $n$ th RIS element, respectively. Since the power of active RIS is supported by an extra energy source, the amplitude  $\beta_n$  can exceed 1, i.e.,  $\tau_n \geq 1$ .  $\boldsymbol{\omega}_r \sim \mathcal{CN}(0, \sigma_r^2 \mathbf{I}_{N \times 1})$  and  $\boldsymbol{\omega}_i \sim \mathcal{CN}(0, \sigma_i^2)$  are the additive white Gaussian noise (AWGN) at the active RIS and the Bob (Eve), respectively.

In ISAC systems, the sensing signal is regarded as interference when decoding the communication signal. To remove the sensing signal before decoding the communication signal, we assume that the received channel fading gain of sensing is stronger than that of the communication at both the Bob and the Eve, which is given by

$$\|\mathbf{g}_i \mathbf{w}_b\|^2 \leq \|\mathbf{g}_i \mathbf{w}_t\|^2, \quad i \in \{b, e\}. \quad (3)$$

Based on (3), the SIC can be explored at both the Bob and the Eve to detect the message of target before decoding the message of Bob.

Based on (2) and (3), the achievable SINR of the Bob decoding the target's signal can be expressed as follows:

$$\text{SINR}_b^t = \frac{\|\mathbf{g}_b \mathbf{w}_t\|^2}{\|\mathbf{g}_b \mathbf{w}_b\|^2 + \sigma_r^2 \|\mathbf{h}_{rb}^H \Theta\|^2 + \sigma_b^2}. \quad (4)$$

If the Bob can successfully decode the target's message, i.e.,  $\text{SINR}_b^t \geq \gamma_t^*$ , where  $\gamma_t^*$  denotes the SINR threshold of the target, the target's signal  $x_t$  can be removed from the received signal at the Bob in (2). Therefore, the achievable SINR of the Bob decodes its own message can be expressed as follows:

$$\text{SINR}_b^b = \frac{\|\mathbf{g}_b \mathbf{w}_b\|^2}{\sigma_r^2 \|\mathbf{h}_{rb}^H \Theta\|^2 + \sigma_b^2}. \quad (5)$$

Based on (2) and (3), the Eve also firstly decodes the target's signal, the corresponding SINR is given by

$$\text{SINR}_e^t = \frac{\|\mathbf{g}_e \mathbf{w}_t\|^2}{\|\mathbf{g}_e \mathbf{w}_b\|^2 + \sigma_r^2 \|\mathbf{h}_{re}^H \Theta\|^2 + \sigma_e^2}. \quad (6)$$

In contrast to Bob, the Eve is constrained to be failed to decode the target's message, i.e.,  $\text{SINR}_e^t < \gamma_t^*$ . In this case, the target's signal is regarded as interference when the Eve decodes the Bob's signal, and the achievable SINR is given by

$$\text{SINR}_e^b = \frac{\|\mathbf{g}_e \mathbf{w}_b\|^2}{\|\mathbf{g}_e \mathbf{w}_t\|^2 + \sigma_r^2 \|\mathbf{h}_{re}^H \Theta\|^2 + \sigma_e^2}. \quad (7)$$

Based on (5) and (7), the secure rate of Bob's signal can be expressed as follows:

$$R_{sec} = [\log_2(1 + \text{SINR}_b^b) - \log_2(1 + \text{SINR}_e^b)]^+, \quad (8)$$

where  $[x]^+ = \max(x, 0)$ .

## B. Sensing Signal Model

According to (1), the received echo signal at the DFBS can be expressed as follows:

$$\mathbf{y}_a = \eta \mathbf{h}_{at} \mathbf{h}_{at}^H (\mathbf{w}_b x_b + \mathbf{w}_t x_t) + \boldsymbol{\omega}_a, \quad (9)$$

where  $\mathbf{h}_{at} = [1, e^{j2\pi d/\lambda \sin(\theta)}, \dots, e^{j2\pi(M-1)d/\lambda \sin(\theta)}]^T$  denotes the channel from the DFBS to the target,  $d$  is antenna spacing,  $\lambda$  is wavelength,  $\theta$  denotes angle of departure,  $\eta$  is the radar cross section (RCS) coefficient with  $\mathbb{E}\{\eta\}^2 = \xi^2$ , and  $\boldsymbol{\omega}_a \sim \mathcal{CN}(0, \sigma_a^2 \mathbf{I}_{M \times 1})$  is the AWGN at the DFBS.

Applying the radar receiver filter  $\mathbf{v} \in \mathbb{C}^{M \times 1}$  at the DFBS, the received echo signal in (9) can be rewritten as follows:

$$\mathbf{v}^H \mathbf{y}_a = \eta \mathbf{v}^H \hat{\mathbf{H}}_t (\mathbf{w}_b x_b + \mathbf{w}_t x_t) + \mathbf{v}^H \boldsymbol{\omega}_a, \quad (10)$$

where  $\hat{\mathbf{H}}_t = \mathbf{h}_{at} \mathbf{h}_{at}^H \in \mathbb{C}^{M \times M}$ .

Both the sensing signal and communication signal can be utilized to detect the sensing target, since the DFBS has knowledge of the echo signals. Based on (10), the SNR of the sensing target at the DFBS is given by

$$\text{SNR}_t = \frac{\xi^2 \mathbf{v}^H \hat{\mathbf{H}}_t (\mathbf{w}_b \mathbf{w}_b^H + \mathbf{w}_t \mathbf{w}_t^H) \hat{\mathbf{H}}_t^H \mathbf{v}}{\sigma_a^2 \mathbf{v}^H \mathbf{v}}. \quad (11)$$

## C. Formulation of Secure Rate Maximization

We aim to maximize the secure rate of Bob's message. The optimization problem of maximizing the secure rate is formulated as follows:

$$\max_{\Theta, \mathbf{v}, \mathbf{w}_b, \mathbf{w}_t} \log_2 \left( 1 + \frac{\|\mathbf{g}_b \mathbf{w}_b\|^2}{\sigma_r^2 \|\mathbf{h}_{rb}^H \Theta\|^2 + \sigma_b^2} \right) \quad (12a)$$

$$\text{s.t. } \|\mathbf{g}_i \mathbf{w}_b\|^2 \leq \|\mathbf{g}_i \mathbf{w}_t\|^2, i \in \{b, e\}, \quad (12b)$$

$$\frac{\|\mathbf{g}_e \mathbf{w}_t\|^2}{\|\mathbf{g}_b \mathbf{w}_b\|^2 + \sigma_r^2 \|\mathbf{h}_{re}^H \Theta\|^2 + \sigma_e^2} \geq \gamma_t^*, \quad (12c)$$

$$\frac{\|\mathbf{g}_e \mathbf{w}_t\|^2}{\|\mathbf{g}_e \mathbf{w}_b\|^2 + \sigma_r^2 \|\mathbf{h}_{re}^H \Theta\|^2 + \sigma_e^2} < \gamma_t^*, \quad (12d)$$

$$\|\mathbf{w}_b\|^2 + \|\mathbf{w}_t\|^2 \leq P_a^{\max}, \quad (12e)$$

$$\|\Theta \mathbf{F}_{ar} \mathbf{w}_b\|^2 + \|\Theta \mathbf{F}_{ar} \mathbf{w}_t\|^2 + \sigma_r^2 \|\Theta\|_F^2 \leq P_r^{\max}, \quad (12f)$$

$$0 \leq \beta_n \leq \tau_n, n = 1, 2, \dots, N, \quad (12g)$$

$$0 < \theta_n \leq 2\pi, n = 1, 2, \dots, N, \quad (12h)$$

$$\frac{\xi^2 \mathbf{v}^H \hat{\mathbf{H}}_t (\mathbf{w}_b \mathbf{w}_b^H + \mathbf{w}_t \mathbf{w}_t^H) \hat{\mathbf{H}}_t^H \mathbf{v}}{\sigma_a^2 \mathbf{v}^H \mathbf{v}} \geq \hat{\gamma}_t^*, \quad (12i)$$

where the optimal variables of the active RIS beamforming  $\Theta$ , the communication transmit beamforming  $\mathbf{w}_b$ , the sensing transmit beamforming  $\mathbf{w}_t$ , and the receive radar beamforming  $\mathbf{v}$  are jointly designed. (12b) represents the SIC decoding order at the Bob and the Eve, (12c) means the target's signal can be correctly detected by the Bob, while (12d) means the Eve cannot successfully decode the target's message, the maximal transmit power of the DFBS with  $P_a^{\max}$  is constrained in (12e), (12f) represents the maximal reflected power of the active RIS with  $P_r^{\max}$ , (12g) and (12h) represent the range of amplitude and phase

shift of the active RIS, respectively, (12i) means the output radar SNR satisfies the worst radar SNR threshold  $\hat{\gamma}_t^*$ .

It can be observed from (12) that the optimal variables  $\Theta$ ,  $\mathbf{v}$ ,  $\mathbf{w}_b$ , and  $\mathbf{w}_t$  are coupled in the objective function and constraint conditions, which is challenging to solve. In this paper, an iterative optimization algorithm based on the MM and SCA are proposed to approximately solve the problem (12).

## III. PROPOSAL SOLUTIONS OF SECURE RATE MAXIMIZATION

In this section, we decompose the original problem (12) into three sub-problems. The first sub-problem is to optimize the receive beamforming  $\mathbf{v}$  at the DFBS, the second sub-problem of designing the active reflection matrix  $\Theta$  of the RIS, and the last sub-problem of joint optimizing the transmit beamforming vectors  $\mathbf{w}_b$  and  $\mathbf{w}_t$ .

### A. Optimizing the Receive Beamforming Vector of DFBS

Fixing the optimal variables  $\Theta$ ,  $\mathbf{w}_b$ , and  $\mathbf{w}_t$ , the original problem (12) about  $\mathbf{v}$  can be rewritten simply as follows:

$$\max_{\mathbf{v}} \frac{\mathbf{v}^H \mathbf{Q} \mathbf{v}}{\mathbf{v}^H \mathbf{v}}, \quad (13)$$

where  $\mathbf{Q} = \xi^2 \hat{\mathbf{H}}_t \mathbf{W} \mathbf{W}^H \hat{\mathbf{H}}_t^H / \sigma_a^2$ , and  $\mathbf{W} = [\mathbf{w}_b, \mathbf{w}_t] \in \mathbb{C}^{M \times 2}$ .

Note that the problem (13) is a typically Rayleigh quotient optimization problem [7], the optimal valuable  $\mathbf{v}^*$  is equivalent to the eigenvector of the largest eigenvalue of the matrix  $\mathbf{Q}$ .

### B. Optimizing the Active Beamforming of RIS

Given the optimal solution of receive beamforming vector, and fixed the transmit beamforming vectors, we aim to design the active beamforming of the RIS based on the original problem (12). Let  $\mathbf{g}_i \mathbf{w}_m = (\mathbf{h}_{ai}^H + \mathbf{h}_{ri}^H \Theta \mathbf{F}_{ar}) \mathbf{w}_m \triangleq \hat{\mathbf{u}}^H \hat{\mathbf{A}}_{im}$ , where  $\hat{\mathbf{u}} = [\hat{u}_1, \dots, \hat{u}_N, 1]^H = [\sqrt{\beta_1} e^{j\theta_1}, \dots, \sqrt{\beta_N} e^{j\theta_N}, 1]^H$ ,  $\hat{\mathbf{A}}_{im} = [\text{diag}(\mathbf{h}_{ri}^H) \mathbf{F}_{ar} \mathbf{w}_m; \mathbf{h}_{ai}^H \mathbf{w}_m]$ ,  $i \in \{b, e\}$ ,  $m \in \{b, t\}$ . Furthermore, let  $\mathbf{U} = \hat{\mathbf{u}} \hat{\mathbf{u}}^H$ ,  $\mathbf{A}_{im} = \hat{\mathbf{A}}_{im} \hat{\mathbf{A}}_{im}^H$ , then  $\|\mathbf{g}_i \mathbf{w}_m\|^2 = \|\hat{\mathbf{u}}^H \hat{\mathbf{A}}_{im}\|^2 = \text{Tr}(\mathbf{U} \mathbf{A}_{im})$ , where  $\text{Tr}(\cdot)$  is trace function. Moreover, let  $\mathbf{h}_{ri}^H \Theta = \hat{\mathbf{u}} \text{diag}(\mathbf{h}_{ri}^H, 0) \triangleq \hat{\mathbf{u}} \hat{\mathbf{H}}_{ri}$ ,  $\mathbf{H}_{ri} = \hat{\mathbf{H}}_{ri} \hat{\mathbf{H}}_{ri}^H$ ,  $i \in \{b, e\}$ , we have  $\|\mathbf{h}_{ri}^H \Theta\|^2 = \text{Tr}(\mathbf{U} \mathbf{H}_{ri})$ , and  $\|\Theta\|_F^2 = \text{Tr}(\mathbf{U}) - 1$ . In addition, let  $\mathbf{g}_{arm} = \mathbf{F}_{ar} \mathbf{w}_m$ , then  $\Theta \mathbf{F}_{ar} \mathbf{w}_m = \text{diag}(\mathbf{g}_{arm}; 0) \hat{\mathbf{u}} \triangleq \hat{\mathbf{G}}_{arm} \hat{\mathbf{u}}$ , where  $\mathbf{G}_{arm} = \hat{\mathbf{G}}_{arm} \hat{\mathbf{G}}_{arm}^H$ , we have  $\|\Theta \mathbf{F}_{ar} \mathbf{w}_m\|^2 = \text{Tr}(\mathbf{U} \mathbf{G}_{arm})$ ,  $m \in \{b, t\}$ .

Now, the original problem (12) can be rewritten as follows:

$$\max_{\mathbf{U}} \log_2 \left( 1 + \frac{\text{Tr}(\mathbf{U} \mathbf{A}_{bb})}{\sigma_r^2 \text{Tr}(\mathbf{U} \mathbf{H}_{rb}) + \sigma_b^2} \right) \quad (14a)$$

$$- \log_2 \left( 1 + \frac{\text{Tr}(\mathbf{U} \mathbf{A}_{eb})}{\text{Tr}(\mathbf{U} \mathbf{A}_{et}) + \sigma_r^2 \text{Tr}(\mathbf{U} \mathbf{H}_{re}) + \sigma_e^2} \right) \quad (14b)$$

$$\text{s.t. } \text{Tr}(\mathbf{U} \mathbf{A}_{ib}) \leq \text{Tr}(\mathbf{U} \mathbf{A}_{it}), i \in \{b, e\}, \quad (14b)$$

$$\text{Tr}(\mathbf{U} \mathbf{A}_{bt}) \geq \gamma_t^* \text{Tr}(\mathbf{U} \mathbf{A}_{bb}) + \gamma_t^* \sigma_r^2 \text{Tr}(\mathbf{U} \mathbf{H}_{rb}) + \gamma_t^* \sigma_b^2, \quad (14c)$$

$$\text{Tr}(\mathbf{U} \mathbf{A}_{et}) < \gamma_t^* \text{Tr}(\mathbf{U} \mathbf{A}_{eb}) + \gamma_t^* \sigma_r^2 \text{Tr}(\mathbf{U} \mathbf{H}_{re}) + \gamma_t^* \sigma_e^2, \quad (14d)$$

$$\text{Tr}(\mathbf{U} \mathbf{G}_{arb}) + \text{Tr}(\mathbf{U} \mathbf{G}_{art}) + \sigma_r^2 (\text{Tr}(\mathbf{U}) - 1) \leq P_r^{\max}, \quad (14e)$$

$$0 \leq \mathbf{U}_{n,n} \leq \tau_n, n = 1, \dots, N, \mathbf{U}_{N+1,N+1} = 1, \quad (14f)$$

$$\mathbf{U} \succeq 0, \quad (14g)$$

$$\text{rank}(\mathbf{U}) = 1. \quad (14h)$$

According to the basic properties of the logarithm function, the object function (14a) can be rewritten as follows:

$$\begin{aligned} R_{sec} = & \log_2 (\text{Tr}(\mathbf{U}\mathbf{A}_{bb}) + \sigma_r^2 \text{Tr}(\mathbf{U}\mathbf{H}_{rb}) + \sigma_b^2) \\ & - \underbrace{\log_2 (\sigma_r^2 \text{Tr}(\mathbf{U}\mathbf{H}_{rb}) + \sigma_b^2)}_{I_2} \\ & - \underbrace{\log_2 (\text{Tr}(\mathbf{U}\mathbf{A}_{eb}) + \text{Tr}(\mathbf{U}\mathbf{A}_{et}) + \sigma_r^2 \text{Tr}(\mathbf{U}\mathbf{H}_{re}) + \sigma_e^2)}_{I_3} \\ & + \log_2 (\text{Tr}(\mathbf{U}\mathbf{A}_{et}) + \sigma_r^2 \text{Tr}(\mathbf{U}\mathbf{H}_{re}) + \sigma_e^2). \end{aligned} \quad (15)$$

Based on MM algorithm [10], the upper bound of the logarithm function  $\log_2(x)$  is given by

$$\log_2(x) \leq \log_2(\hat{x}) + \frac{1}{\hat{x}}(x - \hat{x}), \quad (16)$$

where  $\hat{x}$  is the any given point, and the equality achieved at  $x = \hat{x}$ .

Based on (16), the upper bound of the concave logarithm function of  $I_2$  and  $I_3$  in (15) can be respectively expressed as follows:

$$\begin{aligned} I_2 \leq & \log_2 (\sigma_r^2 \text{Tr}(\mathbf{U}^{(l)}\mathbf{H}_{rb}) + \sigma_b^2) \\ & + \frac{\sigma_r^2 \text{Tr}(\mathbf{U}\mathbf{H}_{rb}) - \sigma_r^2 \text{Tr}(\mathbf{U}^{(l)}\mathbf{H}_{rb})}{\sigma_r^2 \text{Tr}(\mathbf{U}^{(l)}\mathbf{H}_{rb}) + \sigma_b^2}, \end{aligned} \quad (17)$$

and

$$I_3 \leq \log_2 (\mathcal{F}(\mathbf{U}^{(l)}) + \sigma_e^2) + \frac{\mathcal{F}(\mathbf{U}) - \mathcal{F}(\mathbf{U}^{(l)})}{\mathcal{F}(\mathbf{U}^{(l)}) + \sigma_e^2}, \quad (18)$$

where  $\mathbf{U}^{(l)}$  is the  $l$ -th iteration of  $\mathbf{U}$ ,  $\mathcal{F}(\mathbf{U}) = \text{Tr}(\mathbf{U}\mathbf{A}_{eb}) + \text{Tr}(\mathbf{U}\mathbf{A}_{et}) + \sigma_r^2 \text{Tr}(\mathbf{U}\mathbf{H}_{re})$ , and  $\mathcal{F}(\mathbf{U}^{(l)}) = \text{Tr}(\mathbf{U}^{(l)}\mathbf{A}_{eb}) + \text{Tr}(\mathbf{U}^{(l)}\mathbf{A}_{et}) + \sigma_r^2 \text{Tr}(\mathbf{U}^{(l)}\mathbf{H}_{re})$ .

Substituting the upper bounds of  $I_2$  and  $I_3$  in (17) and (18) into (15), and omitting the constant terms in (15), the problem (14) can be rewritten as follows:

$$\begin{aligned} \max_{\mathbf{U}} & \log_2 (\text{Tr}(\mathbf{U}\mathbf{A}_{bb}) + \sigma_r^2 \text{Tr}(\mathbf{U}\mathbf{H}_{rb}) + \sigma_b^2) \\ & + \log_2 (\text{Tr}(\mathbf{U}\mathbf{A}_{et}) + \sigma_r^2 \text{Tr}(\mathbf{U}\mathbf{H}_{re}) + \sigma_e^2) \\ & - \frac{\sigma_r^2 \text{Tr}(\mathbf{U}\mathbf{H}_{rb}) - \sigma_r^2 \text{Tr}(\mathbf{U}^{(l)}\mathbf{H}_{rb})}{\sigma_r^2 \text{Tr}(\mathbf{U}^{(l)}\mathbf{H}_{rb}) + \sigma_b^2} \\ & - \frac{\mathcal{F}(\mathbf{U}) - \mathcal{F}(\mathbf{U}^{(l)})}{\mathcal{F}(\mathbf{U}^{(l)}) + \sigma_e^2} \end{aligned} \quad (19a)$$

$$\text{s.t. } (14b) - (14g). \quad (19b)$$

Note that we relax the constraint  $\text{rank}(\mathbf{U}) = 1$  in (14h), and the convex problem (19) can be efficiently solved by the CVX. If the obtained solutions  $\mathbf{U}^*$  satisfies the rank-1 that is the suboptimal solution. Otherwise, the Gaussian randomization method can be used to obtain the active beamforming vector  $\hat{\mathbf{u}}$ .

### C. Optimizing the Transmit Beamforming Vectors of DFBS

Based on the optimal value  $\mathbf{v}^*$  obtained in problem (13), and the approximated RIS's active beamforming matrix  $\Theta$  in problem (19), we aim to optimize the transmit beamforming vectors  $\mathbf{w}_b$  and  $\mathbf{w}_t$  in problem (12). Let  $\mathbf{H}_t = \hat{\mathbf{H}}_t^H \hat{\mathbf{H}}_t$ ,  $\mathbf{V}^* = \mathbf{v}^* \mathbf{v}^{*H}$ ,  $\hat{\mathbf{H}}_{ar} = \Theta \mathbf{F}_{ar}$ ,  $\mathbf{H}_{ar} =$

$\hat{\mathbf{H}}_{ar}^H \hat{\mathbf{H}}_{ar}$ ,  $\mathbf{G}_i = \mathbf{g}_i^H \mathbf{g}_i$ ,  $i \in \{b, e\}$ , and  $\mathbf{W}_m = \mathbf{w}_m \mathbf{w}_m^H$ ,  $m \in \{b, t\}$ . The original problem (12) can be rewritten as follows:

$$\max_{\mathbf{W}_b, \mathbf{W}_t} \log_2 \left( 1 + \frac{\text{Tr}(\mathbf{G}_b \mathbf{W}_b)}{\sigma_r^2 \|\mathbf{h}_{rb}^H \Theta\|^2 + \sigma_b^2} \right) \quad (20a)$$

$$- \log_2 \left( 1 + \frac{\text{Tr}(\mathbf{G}_e \mathbf{W}_b)}{\text{Tr}(\mathbf{G}_e \mathbf{W}_t) + \sigma_r^2 \|\mathbf{h}_{re}^H \Theta\|^2 + \sigma_e^2} \right) \quad (20b)$$

$$\text{s.t. } \text{Tr}(\mathbf{G}_i \mathbf{W}_b) \leq \text{Tr}(\mathbf{G}_i \mathbf{W}_t), i \in \{b, e\}, \quad (20b)$$

$$\begin{aligned} \text{Tr}(\mathbf{G}_b \mathbf{W}_t) \geq & \gamma_t^* \text{Tr}(\mathbf{G}_b \mathbf{W}_b) + \gamma_t^* \sigma_r^2 \|\mathbf{h}_{rb}^H \Theta\|^2 \\ & + \gamma_t^* \sigma_b^2, \end{aligned} \quad (20c)$$

$$\begin{aligned} \text{Tr}(\mathbf{G}_e \mathbf{W}_t) < & \gamma_t^* \text{Tr}(\mathbf{G}_e \mathbf{W}_b) + \gamma_t^* \sigma_r^2 \|\mathbf{h}_{re}^H \Theta\|^2 \\ & + \gamma_t^* \sigma_e^2, \end{aligned} \quad (20d)$$

$$\text{Tr}(\mathbf{W}_b) + \text{Tr}(\mathbf{W}_t) \leq P_a^{\max}, \quad (20e)$$

$$\begin{aligned} \text{Tr}(\mathbf{H}_{ar} \mathbf{W}_b) + \text{Tr}(\mathbf{H}_{ar} \mathbf{W}_t) & + \sigma_r^2 \|\Theta\|_F^2 \leq P_r^{\max}, \\ & + \xi^2 \text{Tr}(\mathbf{V}^* \mathbf{H}_t \mathbf{W}_b) + \xi^2 \text{Tr}(\mathbf{V}^* \mathbf{H}_t \mathbf{W}_t) \end{aligned} \quad (20f)$$

$$\geq \gamma_t^* \sigma_a^2 \text{Tr}(\mathbf{V}^*), \quad (20g)$$

$$\mathbf{W}_b \succeq 0, \mathbf{W}_t \succeq 0, \quad (20h)$$

$$\text{rank}(\mathbf{W}_b) = \text{rank}(\mathbf{W}_t) = 1. \quad (20i)$$

Based on the basic properties of the logarithm function, the object function (20a) can be rewritten as follows:

$$\begin{aligned} R_{sec} = & \log_2 (\text{Tr}(\mathbf{G}_b \mathbf{W}_b) + \sigma_r^2 \|\mathbf{h}_{rb}^H \Theta\|^2 + \sigma_b^2) \\ & - \log_2 (\sigma_r^2 \|\mathbf{h}_{rb}^H \Theta\|^2 + \sigma_b^2) \\ & - \underbrace{\log_2 (\text{Tr}(\mathbf{G}_e \mathbf{W}_b) + \text{Tr}(\mathbf{G}_e \mathbf{W}_t) + \sigma_r^2 \|\mathbf{h}_{re}^H \Theta\|^2 + \sigma_e^2)}_{Q_1} \\ & + \log_2 (\text{Tr}(\mathbf{G}_e \mathbf{W}_t) + \sigma_r^2 \|\mathbf{h}_{re}^H \Theta\|^2 + \sigma_e^2). \end{aligned} \quad (21)$$

Based on (16), the upper bound of the concave logarithm function of  $Q_1$  in (21) can be expressed as follows:

$$\begin{aligned} Q_1 \leq & \log_2 \left( \mathcal{F}(\mathbf{W}_b^{(l)}, \mathbf{W}_t^{(l)}) + \sigma_r^2 \|\mathbf{h}_{re}^H \Theta\|^2 + \sigma_e^2 \right) \\ & + \frac{\mathcal{F}(\mathbf{W}_b, \mathbf{W}_t) - \mathcal{F}(\mathbf{W}_b^{(l)}, \mathbf{W}_t^{(l)})}{\mathcal{F}(\mathbf{W}_b^{(l)}, \mathbf{W}_t^{(l)}) + \sigma_r^2 \|\mathbf{h}_{re}^H \Theta\|^2 + \sigma_e^2}, \end{aligned} \quad (22)$$

where  $\mathbf{W}_b^{(l)}$  and  $\mathbf{W}_t^{(l)}$  are the  $l$ th iteration of the  $\mathbf{W}_b$  and  $\mathbf{W}_t$ , respectively,  $\mathcal{F}(\mathbf{W}_b^{(l)}, \mathbf{W}_t^{(l)}) = \text{Tr}(\mathbf{G}_b \mathbf{W}_b^{(l)}) + \text{Tr}(\mathbf{G}_e \mathbf{W}_t^{(l)})$ , and  $\mathcal{F}(\mathbf{W}_b, \mathbf{W}_t) = \text{Tr}(\mathbf{G}_b \mathbf{W}_b) + \text{Tr}(\mathbf{G}_e \mathbf{W}_t)$ .

Substituting the upper bound of  $Q_1$  in (22) into (21), omitting the constant term of (21), and the rank-1 constraint in (20i), the non-convex problem (20) can be transformed into a convex problem as follows:

$$\begin{aligned} \max_{\mathbf{W}_b, \mathbf{W}_t} & \log_2 (\text{Tr}(\mathbf{G}_b \mathbf{W}_b) + \sigma_r^2 \|\mathbf{h}_{rb}^H \Theta\|^2 + \sigma_b^2) \\ & + \log_2 (\text{Tr}(\mathbf{G}_e \mathbf{W}_t) + \sigma_r^2 \|\mathbf{h}_{re}^H \Theta\|^2 + \sigma_e^2) \\ & - \frac{\mathcal{F}(\mathbf{W}_b, \mathbf{W}_t) - \mathcal{F}(\mathbf{W}_b^{(l)}, \mathbf{W}_t^{(l)})}{\mathcal{F}(\mathbf{W}_b^{(l)}, \mathbf{W}_t^{(l)}) + \sigma_r^2 \|\mathbf{h}_{re}^H \Theta\|^2 + \sigma_e^2} \end{aligned} \quad (23a)$$

$$\text{s.t. } (20b) - (20h). \quad (23b)$$

**Algorithm 1:** The Iterative Algorithm for Solving Problem (12).

- 1: **Initialize:** Set the beamforming vectors  $\mathbf{w}_t = \mathbf{w}_b = \mathbf{1}_{M \times 1}$ , secrecy rate  $R = 0$ , reflection coefficient matrix  $\Theta = \mathbf{I}_N$ , and the convergence tolerance  $\delta = 10^{-4}$ .
- 2: **repeat**
- 3:   Obtain  $\mathbf{v}^*$  via solving problem (13).
- 4:   Obtain  $\mathbf{U}^*$  via solving problem (19). Then the Gaussian randomization is applied to construct the rank-one solution, and update  $\Theta^*$ .
- 5:   Obtain  $\mathbf{W}_t^*, \mathbf{W}_b^*$  via solving problem (23) with  $\Theta^*, \mathbf{v}^*$ . Then the Gaussian randomization is used to construct the rank-one solution, and update  $\mathbf{w}_t^*, \mathbf{w}_b^*$ .
- 6:   Calculate (12a) and assign the value to  $R^*$ .
- 7:   Update  $\Theta \leftarrow \Theta^*$ ,  $\mathbf{v} \leftarrow \mathbf{v}^*$ ,  $\mathbf{w}_t \leftarrow \mathbf{w}_t^*$ ,  $\mathbf{w}_b \leftarrow \mathbf{w}_b^*$ , and  $R \leftarrow R^*$ .
- 8: **until**  $|R^* - R| \leq \delta$ .

The tool of CVX can be used to solve the problem (23).

The iterative algorithm for solving problem (12) is summarized in Algorithm 1, where  $\delta$  denotes the convergence criteria of the algorithm. Initially, given the beamforming vectors  $\mathbf{w}_t = \mathbf{w}_b = \mathbf{1}_{M \times 1}$ , secrecy rate  $R = 0$ , and reflection coefficient matrix  $\Theta = \mathbf{I}_N$ . The initial setting of feasible points that satisfy all constraint conditions at the beginning of the algorithm can ensure that the algorithm trends towards quick convergence. Firstly, the vector  $\mathbf{v}^*$  can be obtained based on (13). Subsequently, solving problem (19), the approximated optimal solution  $\mathbf{U}^*$  can be obtained, and  $\Theta^*$  is updated. Finally, using the updated  $\Theta^*$  and  $\mathbf{v}^*$ , the beamforming vectors  $\mathbf{w}_t^*$ , and  $\mathbf{w}_b^*$  can be derived by solving problem (23). The iteration process continues until the convergence condition is satisfied.

The complexity of updating the receiver beamforming  $\mathbf{v}$  in (13) is  $\mathcal{O}(M^3)$ . The SDP is applied to update the active RIS beamforming  $\Theta$  in (19), and the transmit beamforming vectors  $\mathbf{w}_b$  and  $\mathbf{w}_t$  in problem (23), the corresponding computation complexity are  $\mathcal{O}(N^{4.5}) \log(\epsilon^{-1})$  and  $\mathcal{O}(M^{3.5}) \log(\epsilon^{-1})$ , respectively, where  $\epsilon$  is the accuracy tolerance. Therefore, the overall complexity of problem (12) is  $\mathcal{O}(M^{3.5} + N^{4.5}) \log(\epsilon^{-1})$ .

#### IV. SIMULATION RESULTS

In this section, the numerical results are provided to evaluate the secure rate of the proposed ISAC systems aided by active RIS. For illustration, the simulation parameters are settled as  $\sigma_e^2 = \sigma_b^2 = \sigma_r^2 = -80$  dBm [4],  $\gamma_t^* = 0.6$ ,  $\xi = 1$ ,  $d_{ar} = d_{ab} = d_{rb} = 90$  m,  $d_{ae} = 200$  m, and  $d_{re} = 150$  m. The distance-related path-loss function is modelled as  $L(d)$  (in dB)=  $35.1 + 36.7 \lg(d) - G_t - G_r$  [11], where  $G_t = 10$  dBi and  $G_r = 10$  dBi denote the antenna gains of the transmitter and receiver, respectively.

We present the secure rate versus the maximal transmit power  $P_a^{\max}$  under three different schemes in Fig. 2, where the maximal transmit power of the passive RIS is given as  $P_a^{\max} + P_r^{\max}$  for fairness. It can be observed from Fig. 2 that the active RIS can achieve higher secure rate than that of the passive RIS for the ISAC systems. This is because the active RIS with controllable amplitude can achieve the benefit of channel enhancement, compared to the passive RIS. Furthermore, the active RIS with reflected power can enable to amplify the power of reflected signals towards the destination, which can further improve the communication performance by strengthening signal propagation. In addition, we can observe that the secure rate of the proposed active RIS-assisted ISAC systems outperforms the active RIS-assisted

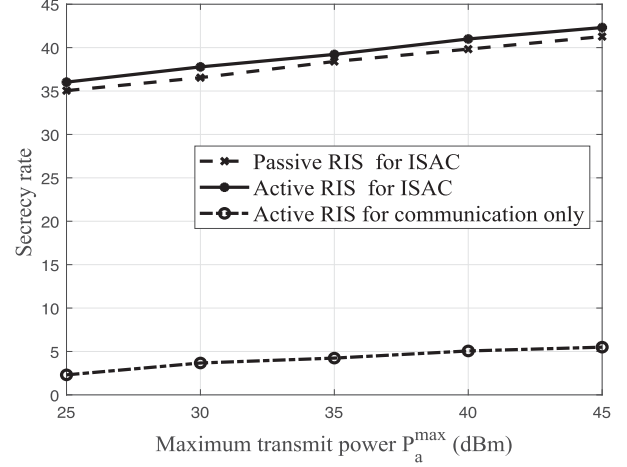


Fig. 2. Impact of  $P_a^{\max}$  on secure rate for different schemes, where  $N = 20$ ,  $M = 3$ ,  $\tau_n = 15$  dB,  $\forall n$ , and  $P_r^{\max} = 20$  dBm.

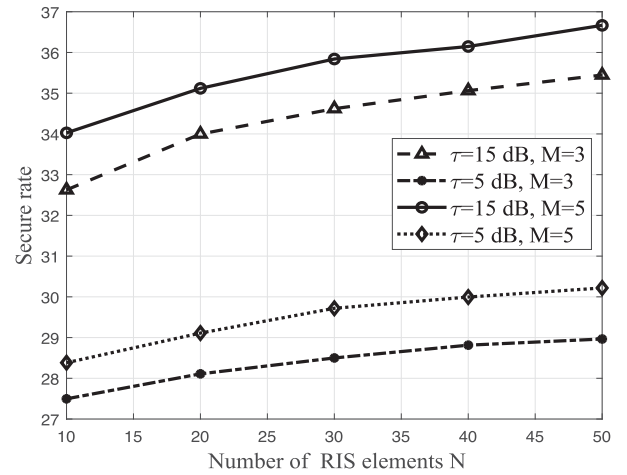


Fig. 3. Impact of  $N$  on secure rate for the ISAC systems aided by active RIS, where  $P_a^{\max} = P_r^{\max} = 20$  dBm, and  $\tau = \tau_n, \forall n$ .

communication-only systems. The main reason is that the target is considered as a cooperative jamming in the proposed scheme, which can remarkably decrease the achievable rate of the Eve without impacting the achievable rate of the Bob.

The impact of the active RIS's reflecting units  $N$  on secure rate in active RIS-aided ISAC systems is shown in Fig. 3. It can be seen that the secure rate is an increasing function of  $N$ . Furthermore, it can be also observed that increasing the amplitude of the active RIS can contribute to increasing the secure rate of the ISAC systems aided by active RIS. This can be explained that the larger amplitude capability of the active RIS can indeed have a significant impact on enhancing the channel condition and improving the secrecy performance. In addition, increasing the number of the antennas can contribute to improving the secure rate, as a larger number of transmit antennas can provide higher spatial degrees of freedom.

Fig. 4 shows the convergence behaviour of Algorithm 1. It can be observed that the secure rate of the proposed algorithm converges quickly after a small number of iterations, illustrating the feasibility of the proposed algorithm.

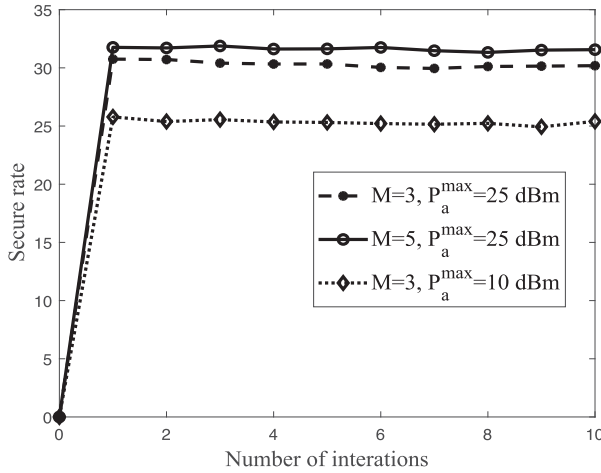


Fig. 4. Convergence behaviour of the proposed iterative Algorithm 1, where  $P_r^{\max} = 20$  dBm,  $\tau_n = 10$  dB, and  $N = 20$ .

## V. CONCLUSION

In this paper, we investigated the secure rate maximization problem for the active RIS-assisted ISAC systems, where the transmit beamformers, the active RIS refection matrix, and the radar receive beamformer were jointly designed. A low complexity alternation optimization algorithm based on SCA and MM were proposed to maximize the secure rate. Simulation results demonstrated the significant benefits of integrating sensing with communication using active RIS to improve the secure rate, compared to the active RIS is solely used for communication purposes. For future works, the secrecy performance of ISAC systems assisted by active RIS with imperfect CSI arises as an interesting open problem, in which the linear minimal mean square error estimator can be utilized to accurately estimate the cascaded channel for the active RIS.

## REFERENCES

- [1] Y. Zhang et al., "STAR-RIS assisted secure transmission for downlink multi-carrier NOMA networks," *IEEE Trans. Inf. Forensics Secur.*, vol. 18, pp. 5788–5803, 2023.
- [2] F. Liu, C. Masouros, A. P. Petropulu, H. Griffiths, and L. Hanzo, "Joint radar and communication design: Applications, state-of-the-art, and the road ahead," *IEEE Trans. Commun.*, vol. 68, no. 6, pp. 3834–3862, Jun. 2020.
- [3] L. Dong, H.-M. Wang, and J. Bai, "Active reconfigurable intelligent surface aided secure transmission," *IEEE Trans. Veh. Technol.*, vol. 71, no. 2, pp. 2181–2186, Feb. 2022.
- [4] S. Fang, G. Chen, P. Xu, J. Tang, and J. A. Chambers, "SINR maximization for RIS-assisted secure dual-function radar communication systems," in *Proc. IEEE Glob. Commun. Conf.*, Madrid, Spain, 2021, pp. 1–6.
- [5] H. Zhao, F. Wu, W. Xia, Y. Zhang, Y. Ni, and H. Zhu, "Joint beamforming design for RIS-aided secure integrated sensing and communication systems," *IEEE Commun. Lett.*, vol. 27, no. 11, pp. 2943–2947, Nov. 2023.
- [6] C. Jiang, C. Zhang, C. Huang, J. Ge, J. He, and C. Yuen, "Secure beamforming design for RIS-assisted integrated sensing and communication systems," *IEEE Wireless Commun. Lett.*, vol. 13, no. 2, pp. 520–524, Feb. 2024.
- [7] Q. Zhu, M. Li, R. Liu, and Q. Liu, "Joint transceiver beamforming and reflecting design for active RIS-aided ISAC systems," *IEEE Trans. Veh. Tech.*, vol. 72, no. 7, pp. 9636–9640, Jul. 2023.
- [8] A. A. Salem, M. H. Ismail, and A. S. Ibrahim, "Active reconfigurable intelligent surface-assisted MISO integrated sensing and communication systems for secure operation," *IEEE Trans. Veh. Technol.*, vol. 72, no. 4, pp. 4919–4931, Apr. 2023.
- [9] X. Wang, Z. Fei, Z. Zheng, and J. Guo, "Joint waveform design and passive beamforming for RIS-assisted dual-functional radar-communication system," *IEEE Trans. Veh. Technol.*, vol. 70, no. 5, pp. 5131–5136, May 2021.
- [10] Y. Sun, P. Babu, and D. P. Palomar, "Majorization-minimization algorithms in signal processing, communications, and machine learning," *IEEE Trans. Signal Process.*, vol. 65, no. 3, pp. 794–816, Feb. 2017.
- [11] L. Lv, Q. Wu, Z. Li, Z. Ding, N. Al-Dhahir, and J. Chen, "Covert communication in intelligent reflecting surface-assisted NOMA systems: Design, analysis, and optimization," *IEEE Trans. Wireless Commun.*, vol. 21, no. 3, pp. 1735–1750, Mar. 2022.